

Dielectric sample testing for ceramic insert in high-pressured cavity

Huy Phan,* Katsuya Yonehara, and Ben Freemire
Fermilab, Batavia, IL
(Dated: August 18, 2014)

Recent design for helical cooling channel of a muon accelerator requires that the cavities are fully enclosed inside solenoids and other magnetic components; therefore, it is optimal that we can reduce the RF cavity's radius. One of the possible solution is to introduce a ceramic ring into the cavity, partially loading it with dielectric and reducing the radius needed to achieved the same resonant frequency. We have conducted a sample test to determine the characteristics of various dielectric materials. Our method is to put dielectric sample inside a test cavity and measure the cavity's characteristics. By comparing our measurements with POISSON/SUPERFISH simulation results, we can find the dielectric constant ϵ and loss tangent $\tan\delta$ of the sample. Alumina 99.5%, which $\epsilon=9.5$ and $\tan\delta=0.00012$, appears to be one of the best candidates to be the insert ring's material. However, there are still some disagreement about our calculated loss tangent and expected values. This paper will discuss our sample test result and how to improve it in the future.

I. INTRODUCTION

One of the technical challenges for realization of a muon collider is how to effectively cool down the muon beam and reduce excessive momentum spread. As of now, ionization cooling is the most realistic approach considering the short lifetime of muon particle. Ionization cooling involves letting the beam passes through some absorber in order to decrease the beam transverse momentum via ionization. As a result, the longitudinal phase space is increased in the process, but this heating effect can be reduced by introducing dispersion to the system. The current design for the helical cooling channel uses high-pressured gas-filled RF cavities contained within complicated magnet systems which provide necessary dispersion for emittance exchange. Therefore, it is optimal to minimize the radial size of the cavities in order to fit into the magnet systems. One recent proposal suggests to insert a ceramic ring into the RF cavity, as loading the cavity with dielectric will reduced the required cavity's radius for a given resonant frequency:

$$f_{010} \propto \frac{1}{R\sqrt{\mu\epsilon}}. \quad (1)$$

Partially loading the cavity with dielectric material however results in drop of quality factor, thus it is necessary to choose appropriate material that can effectively reduce the cavity radius with minimal efficiency loss. We have conducted experiments to determine the dielectric constant and loss tangent of various materials to be used as the insert ring. This paper will discuss our experimental results and further preparation for future MTA beam test.

II. DIELECTRIC INSERT RING IN HIGH-PRESSURED GAS-FILLED CAVITY

A. Ionization cooling in helical cooling channel

In addition to short lifetime, muon bunches, when created via pion decay, have large volume, angular spread and energy spread, making practical usage in an accelerator impossible. So far, only ionization cooling offers a way to effectively lower the bunch's 6D phase space within acceptable time. In this cooling scheme, muon beam passes through a low-Z absorber and loses both of its transverse and longitudinal momentum via ionization[1]. The lost longitudinal momentum is then recovered by RF cavities. The normalized transverse emittance of such beam within a lattice is

$$\frac{d\epsilon_n}{ds} = \frac{-1}{\beta^2} \left\langle \frac{dE}{ds} \right\rangle \frac{\epsilon_n}{E} + \frac{1}{\beta^3} \frac{\beta_{\perp}(0.014)^2}{2EmL_R} \quad (2)$$

where s is the path length; β is ratio between muon velocity and speed of light; E is muon energy(GeV); m is muon mass(GeV/ c^2); β_{\perp} is the lattice betatron function and L_R is radiation length of the absorber.

The first term of Eq.2 represents the ionization cooling process while the second term indicates heating effect by scattering. However, this cooling process only lowers transverse phase space, hence emittance exchange (transferring cooling effect to longitudinal phase space) is required. Emittance exchange can be accomplished by utilizing the magnet system of solenoids, helical dipoles and helical quadrupole magnetic field components in the helical cooling channel(HCC). The helical magnetic system will provide necessary dispersion for the beam to reduce its longitudinal phase space; however, the transverse phase space is increased as a result, making 6D cooling possible.[2]

* Physics Department, McDaniel College.

B. Dielectric insert ring

In HCC design, gas-filled cavities are entirely enclosed within the helical magnet systems, thus it is optimal to reduce the cavities' radial size. It is proposed that a ceramic ring should be placed inside the cavity to increase its relative permittivity ϵ , which, according to Eq.1, decreases the necessary radius to achieve the same resonant frequency(Fig.1). For a cavity fully loaded with relative permittivity 9.6, we can achieve a size reduction of 3 times the radius[3]. Since we only put an insert ring instead of filling the cavity with dielectric, the reduction capability is estimated to be around 1.4 for the same dielectric constant(relative permittivity).

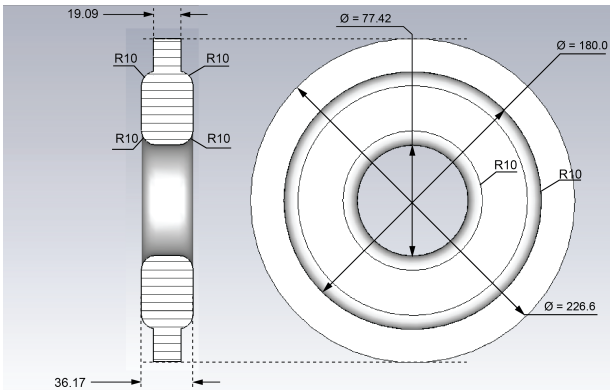


FIG. 1: Dielectric insert design for high-pressed RF cavity. This doughnut-shaped insert will be held into the cavity by teflon structure.

Initially, there are several issues with introducing dielectric material inside an RF cavity. Power dissipated inside the ceramic contributes significantly to the loss in cavity efficiency. Dielectric heating per unit volume generated by an electric field depends on the relative permittivity and loss tangent of the material:

$$\frac{dP}{dV} = 2\pi f \epsilon' \tan\delta E^2 \quad (3)$$

where f is the frequency of the field, ϵ' the real component of permittivity, $\tan\delta$ the loss tangent and E the electric field. For high-powered cavity capable of reaching 20MV/m peak gradient at 500MHz, low loss tangent material like alumina might dissipate up to around $15000\text{W}/\text{cm}^3$ (Fig.2). Aside from apparent loss in cavity power, dielectric heating can also damage the ceramic ring because of consequential thermal stress. Furthermore, dielectric structure tends to cause surface breakdown in the cavity.

Despite several shortcomings, the dielectric ring is not as intrusive in hydrogen-filled pressurized cavity as it is in a vacuum cavity. For instances, the gas acts as momentum absorber for the beam and coolant for the heating ceramic ring. Extensive study on gas-filled cavity also shows that the presence of gaseous hydrogen can inhibit

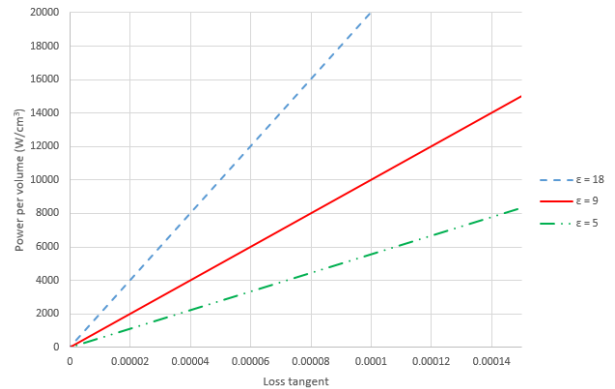


FIG. 2: Volumetric power dissipation versus loss tangent of dielectric material of varying dielectric constant. Example materials corresponding to $\epsilon=5,9,18$ are pyrex, alumina and magnesium calcium titanate respectively.

breakdown events. As such, it is technically reasonable to use dielectric ring for cavity's size reduction.

III. DIELECTRIC SAMPLE TEST

A. Experimental setup

The main goal of our dielectric sample test is to precisely measure the dielectric constant and loss tangent of potential ceramic ring materials. Most of our focus is on alumina(Al_2O_3) because of its suitable dielectric constant(9.0 ~ 10.0) and low loss tangent(~ 0.0001). Our samples include alumina (94%, 96%, 97.6%, 99.5%, and 99.8% purity), magnesium calcium titanate(MCT), aluminum nitride (AlN) and cordierite ($(\text{Mg}, \text{Fe})_2\text{Al}_4\text{Si}_5\text{O}_8$), in either cylindrical rod or tube shape(Fig.3).



FIG. 3: Alumina tube samples with different purity. Alumina 300: 94% purity; Alumina 500: 96% purity; Alumina 600: 97.6%; Alumina 995: 99.5%.

The samples are to be placed inside a test cavity on the electrode through a hole in the top plate, which can be covered by a copper plunger(Fig.4). A small spring is embedded around the perimeter of the plunger to ensure good contact with the top plate. Furthermore, the plunger can be connected to the top plate through multiple threads, along with a number of bolts and washers to secure the plunger. The actual dimension of the



(a) Test cavity

(b) Network analyzer

FIG. 4: Experimental setup with a test cavity connecting to a network analyzer

cavity and its components are illustrated in Fig.5. As we receive samples from multiple vendors, they all have different lengths and radii. We measure the quality factor and resonant frequency of the cavity by connecting it to a network analyzer via two cable pickups. By comparing our experimental measurement with simulation in POISSON/SUPERFISH program, we can determine the dielectric constant and loss tangent of the sample.

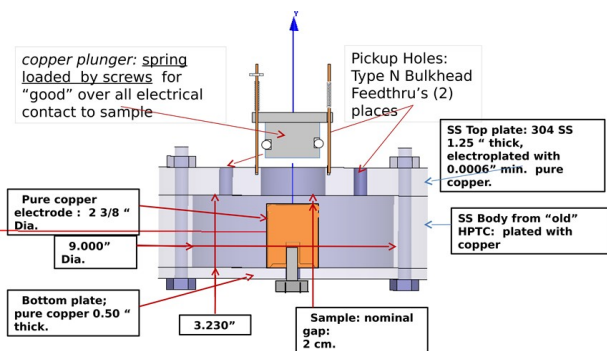


FIG. 5: Test cavity design. The actual length of the cavity is 1.45mm longer than shown in diagram.

POISSON/SUPERFISH is a problem-solving program cowritten by Ron Holsinger and Klaus Halbach to calculate electromagnetic field and resonant frequency inside axially symmetrical RF cavity. Along with the cavity's geometry, dielectric constant and loss tangent of involved material are required parameters for the program's input file. Changing these parameters results in a different output electromagnetic field, quality factor and resonant frequency for the given geometry. Thus it is possible to simulate the relationship between cavity's measurements and material's properties.

B. Experimental procedure

Since the program assumes ideal resistivity for copper wall, it supposes to create a shift between simulation result and measurement data(Fig.7). In order to verify the effect of wall resistivity, we take measurements of quality factor using an empty cavity with different plunger depth(how far the plunger goes in the cavity) and compare them with simulation result from corresponding geometry(Fig.6).

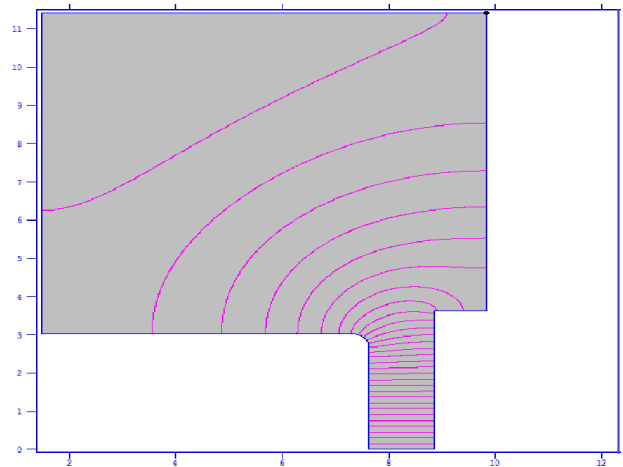


FIG. 6: POISSON/SUPERFISH simulation of empty cavity. The protruding white rectangular from the right side represents the copper plunger.

There is indeed a systematic shift between measurements and simulation data because of actual resistivity of the wall and connection between component copper plates. However, the fact that the cavity is 1.45mm longer than it should be contributes to this discrepancy as well. Further investigation involves using simulation result of the empty cavity and its actual measurement to determine the copper wall resistivity, which is proportional to the square of the ratio of simulated quality factor (using ideal resistivity) and actual quality factor:

$$\rho_{sim} = \left(\frac{Q_{sim}}{Q_{meas}} \right)^2 \rho_{ideal}. \quad (4)$$

The wall resistivity is found to be $3.16 \times 10^{-6}(\Omega m)$, comparing to ideal resistivity of copper $1.72 \times 10^{-6}(\Omega m)$ (Fig.8). As expected, using this value results in quality factor of 11135.2, whereas the actual measurement of the same empty cavity is 11135.187.

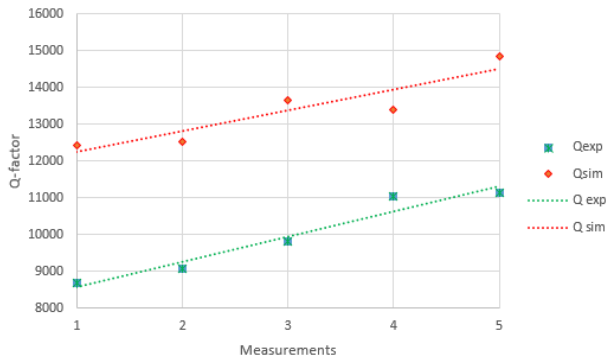


FIG. 7: Comparison between simulated quality factor and experimental quality factor. Simulation results are higher than the actual measurement because we use ideal resistivity for the wall.

Each sample is wiped with alcohol before being placed at the center of the electrode as precisely as possible. We then slowly squeeze the plunger into the cavity until it reaches the sample. To ensure good contact, we secure the plunger with threads and tighten the wing nuts lightly afterward. Also, the plunger's depth is recorded for more accurate geometry in simulation. Short, open and load calibration for pickups are performed after each measurement to maintain accurate reflection feedback with the help of type-N calibration kit.

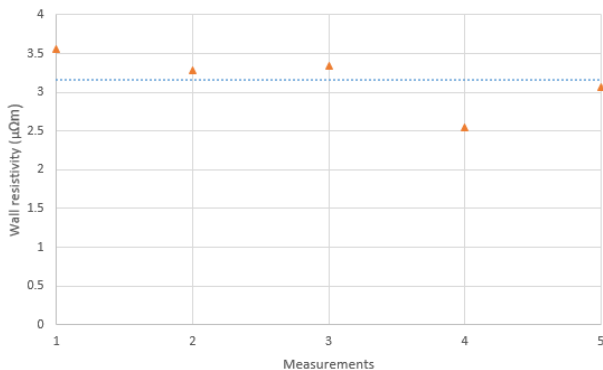


FIG. 8: Calculated wall resistivity for 5 measurements of different sample-less setups. The plunger depth varies with each setup, creating a discrepancy in calculated wall resistivity. The average line has value $3.16\mu\Omega m$.

For cavity's characteristics measurements, we connect the two pickup probes into network analyzer ports and observe resonant peak. The resonant of frequency can be read by placing a marker on top of the peak. However, the network analyzer only displays the loaded quality factor, thus it is necessary to calculate the actual quality factor using the probes' impedance, which can be measured during calibration process

$$Q = Q_L \left(1 + \frac{R_{01} + R_{02}}{50} \right), \quad (5)$$

where Q_L is the displayed quality factor, and R_{01} and R_{02} are the probes' impedances.

IV. RESULT AND DISCUSSION

A. POISSON/SUPERFISH simulation

Simulation by POISSON/SUPERFISH(Fig.9) shows that there is a linear relationship between the sample's dielectric constant and the cavity's resonant frequency(Fig.11). In contrast, the loss tangent only has minimal influence to the frequency. This result is within expectation as part of the electric field power is stored within the dielectrics, reducing the cavity's efficiency. For similar reason, the quality factor also decreases as dielectric constant and resonant frequency increases, albeit non-linearly(Fig.12).

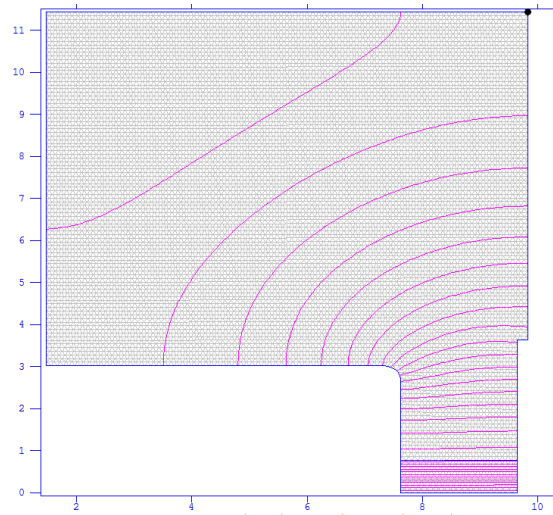


FIG. 9: POISSON/SUPERFISH simulation of the cavity with dielectric sample. The color lines are vector potential within the cavity.

One possible issue for our test is the sensitivity of measurements to the gap between the plunger and the sample. If there is a small air gap between the sample and the plunger, the cavity's resonant frequency will be shifted by a considerable amount. It only takes a gap of 0.23mm to offset the resonant frequency by 1MHz(Fig.10). Repeated contacts with the sample or excessively rough handling can slightly deform the copper plunger or sample, thus creating such thin gap.

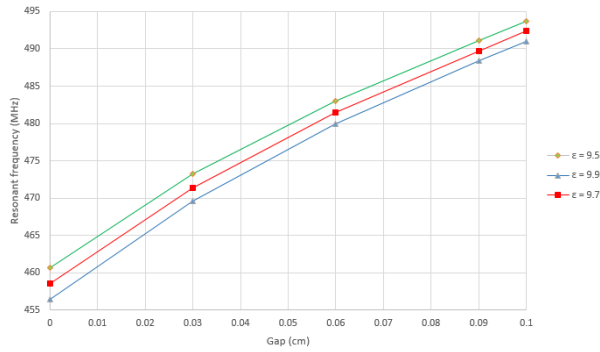


FIG. 10: How small gap between plunger and sample affects resonant frequency of the cavity. The value at 0cm gap is when the plunger makes ideal contact with the sample.

In order to make sure good contact, we put wing nuts on the connecting thread between the plunger and the top plate, above the plunger. By tightening the nuts slowly, we apply a steady downward pressure onto the plunger, closing in any thin gap that might present.

B. Test result

Our calculated dielectric constant closely follows the values given by the manufacturing vendors, having below 6% error for each sample. The discrepancy is highest for the MCT sample, with measured value at 18.89 comparing to provided value of 20. For aluminum nitride sample, we measure a dielectric constant of 8.54; but as the vendor does not provide any value for this sample, we use the dielectric constant of 9, according to www accuratus.com, as our accepted value. This value results in a 4.8% error for aluminum nitride sample.

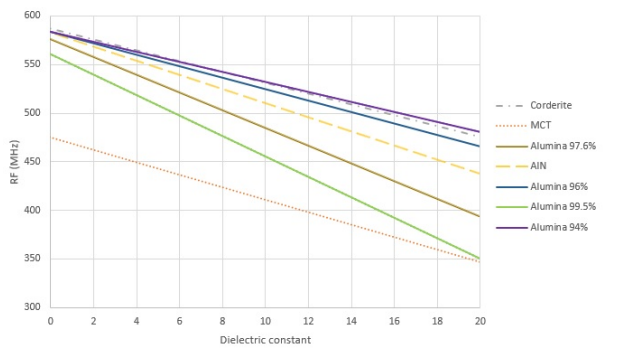


FIG. 11: Resonant frequency versus dielectric constant for different samples. Since the frequency is only minimally dependent on loss tangent, we can compare the measured resonant frequency with the simulation to directly determine the samples' dielectric constant.

Calculation using corderite sample yields a dielectric constant of 4.52 comparing to provided value of 4.6, which corresponds to a 1.7% error. All the measurements

for alumina samples shows that the dielectric constants are between 8.5 ~ 9.5 for given purities. Each of them has error below 3.5% from the provided values(Fig.13).

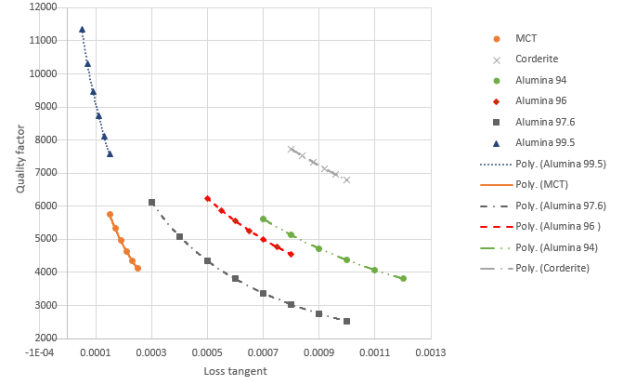


FIG. 12: Simulated relationship between quality factor and loss tangent for each sample. Note that the simulation uses determined dielectric constant, calculated by comparing simulated resonant frequency vs dielectric constant plot and measured frequency .

In contrast to our dielectric constant results, measured loss tangents for alumina samples are more offset from vendor-provided values(Fig.14). While results for alumina 99.5% are fairly close to provided values, the other samples' loss tangents are lower than expected by a significant amount.

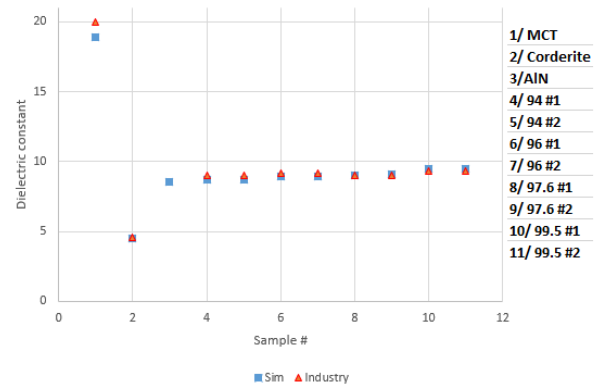


FIG. 13: Calculated dielectric constant and given dielectric constant for each sample. The vendor manufacturing aluminum nitride sample does not provide specific value for its dielectric constant.

Non-alumina samples like MCT, corderite and aluminum nitride do not have any industry-provided loss tangent values. Nonetheless, the obtained loss tangents for both MCT and corderite sample are around 0.0012, which is higher than alumina's as expected. In addition, aluminum nitride sample has much higher loss tangent than any other materials at 0.018. Calculation for alumina 99.5% yields loss tangent of 0.00011 for first sample

and 0.00013 for second sample, comparing with the given value of 0.00014. The mean error for alumina 99.5% is approximately 14%. This discrepancy increases as the purity of the sample drops. For instances, the mean error is 29% for alumina 97.6% samples, 35% for alumina 96% and 37% for alumina 94%.

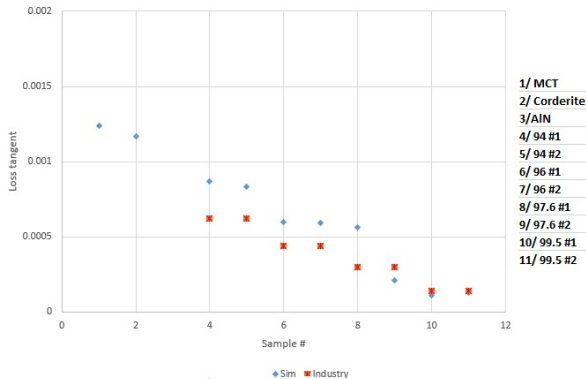


FIG. 14: Calculated loss tangent and given loss for each sample. Non-alumina samples' loss tangent are not specified by their manufacturers. Aluminum nitride sample has a really high loss tangent value of 0.018, therefore it is not shown in the graph for display purpose.

However, such discordance might not mean faulty in calculation or experimental technique. It is possible that the vendors have tested these samples under a different frequency instead of 200MHz. In addition, there are also issues of damage or degradation of material over time that might affect the samples' loss tangent. Another reason is that there might be unaccounted resistivity on the copper wall. The cavity is assembled using 2 copper plates and a pillbox cavity body, along with a copper plunger, so there will be connecting surfaces between each component that can contribute significantly to the wall's extra resistivity. This issue can be solved by revise how we model the cavity in POISSON/SUPERFISH by adding extra materials with more prominent resistivity in between connected areas.

As shown in Eq.3, dissipated power depends on both dielectric constant and loss tangent, hence there are trade-off between cavity's performances and size reduction capability. In that case, alumina 95% seems to be the one of the most suitable candidates for the ring's material since it has a well balance between dielectric constant and loss tangent. Furthermore, product between dielectric constant and loss tangent yields the smallest value for alumina in general(Fig.15).

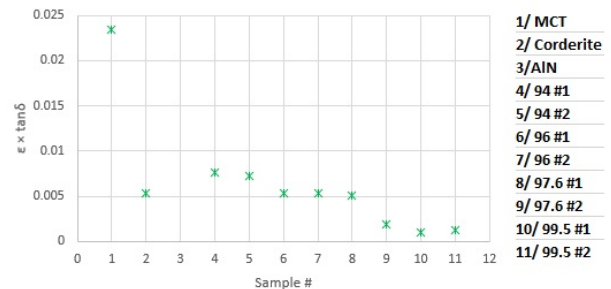


FIG. 15: Product between dielectric constant and loss tangent for each sample. Aluminum nitride's value is saturated and will not be shown for display purpose.

V. CONCLUSION

We successfully found the dielectric constant and loss tangent of potential materials for the dielectric insert. While our calculated dielectric constants agree well with provided values from the vendors, having below 6% error for all samples, the results for loss tangent experience a discrepancy with regard to provided values. As the purity of alumina decreases, the difference between measured and expected values increases. We speculate that there are two possible reasons for such error. As the loss tangent varies with frequencies, the manufacturer might have used a different frequency from the one that we used (200MHz). In addition, there might be extra resistivity on the cavity's wall that we were not aware of, thus hindering our ability to model the cavity correctly. To better represent the cavity, we propose adding thin layers of metal with significant resistivity between connecting components. By adjusting the resistivity of those layers to match simulation with actual measurement, we can figure out the actual resistivity of the wall. Overall, alumina 99.5% shows to be the best candidate so far with $\epsilon \approx 9.5$ and $tand \approx 0.00012$.

VI. REFERENCES

- [1] K.Yonehara et al., "A helical cooling channel system for muon collider", *Proceeding IPAC-2010*
- [2] R.Palmer et al., "Ionization cooling ring for muons", *Physical Review Special Topics - Accelerator and Beams* **8**, 2005
- [3] L.M.Nash et al., "High power tests of alumina in high pressure RF cavities for muon ionization cooling channel", 2011.